


Muscle Transcriptomics Shows Overexpression of Cadherin 1 in Inclusion Body Myositis

Chiseko Ikenaga, MD, PhD ^{1,2}, Hidetoshi Date, PhD,³ Motoi Kanagawa, PhD,^{4,5}
Jun Mitsui, MD, PhD,⁶ Hiroyuki Ishiura, MD, PhD,¹ Jun Yoshimura, PhD,⁷
Iago Pinal-Fernandez, MD, PhD,^{2,8,9} Andrew L. Mammen, MD, PhD,^{2,8}
Thomas E. Lloyd, MD, PhD,^{2,10} Shoji Tsuji, MD, PhD,^{6,11} Jun Shimizu, MD, PhD,^{1,12}
Tatsushi Toda, MD, PhD,^{1,4} and Jun Goto, MD, PhD^{13,14}

Objective: This study aimed to elucidate the molecular features of inclusion body myositis (IBM).

Methods: We performed RNA sequencing analysis of muscle biopsy samples from 67 participants, consisting of 58 myositis patients with the pathological finding of CD8-positive T cells invading non-necrotic muscle fibers expressing major histocompatibility complex class I (43 IBM, 6 polymyositis, and 9 unclassifiable myositis), and 9 controls.

Results: Cluster analysis, principal component analysis, and pathway analysis showed that differentially expressed genes and pathways identified in IBM and polymyositis were mostly comparable. However, pathways related to cell adhesion molecules were upregulated in IBM as compared with polymyositis and controls ($p < 0.01$). Notably, *CDH1*, which encodes the epidermal cell junction protein cadherin 1, was overexpressed in the muscles of IBM, which was validated by another RNA sequencing dataset from previous publications. Western blotting confirmed the presence of mature cadherin 1 protein in the muscles of IBM. Immunohistochemical staining confirmed the positivity for anti-cadherin 1 antibody in the muscles of IBM, whereas there was no muscle fiber positive for anti-cadherin 1 antibody in immune-mediated necrotizing myopathy, antisynthetase syndrome, and controls. The fibers stained with anti-cadherin 1 antibody did not have rimmed vacuoles or abnormal protein accumulation. Experimental skeletal muscle regeneration and differentiation systems showed that *CDH1* is expressed during skeletal muscle regeneration and differentiation.

Interpretation: *CDH1* was detected as a differentially expressed gene, and immunohistochemistry showed that cadherin 1 exists in the muscles of IBM, whereas it was rarely seen in those of other idiopathic inflammatory myopathies. Cadherin 1 upregulation in muscle could provide a valuable clue to the pathological mechanisms of IBM.

ANN NEUROL 2022;91:317–328

View this article online at [wileyonlinelibrary.com](https://onlinelibrary.wiley.com/doi/10.1002/ana.26304). DOI: 10.1002/ana.26304

Received Oct 16, 2021, and in revised form Jan 18, 2022. Accepted for publication Jan 19, 2022.

Address correspondence to Dr Ikenaga, Department of Neurology, Johns Hopkins University School of Medicine, Pathology Building 537, 600 North Wolfe Street, Baltimore, MD 21205; E-mail: cikenaga-ty@umin.ac.jp and Dr Goto, Department of Neurology, International University of Health and Welfare, Ichikawa Hospital, 6-1-14 Konodai, Ichikawa, Chiba, 272-0827, Japan; E-mail: gotoj-ty@umin.ac.jp

From the ¹Department of Neurology, Graduate School of Medicine, The University of Tokyo, Tokyo, Japan; ²Department of Neurology, Johns Hopkins University School of Medicine, Baltimore, MD, USA; ³Department of Neurology, National Center Hospital, National Center of Neurology and Psychiatry, Tokyo, Japan; ⁴Division of Molecular Brain Science, Kobe University Graduate School of Medicine, Kobe, Japan; ⁵Department of Cell Biology and Molecular Medicine, Ehime University Graduate School of Medicine, Ehime, Japan; ⁶Department of Molecular Neurology, Graduate School of Medicine, The University of Tokyo, Tokyo, Japan; ⁷Department of Computational Biology and Medical Sciences, Graduate School of Frontier Sciences, The University of Tokyo, Chiba, Japan; ⁸Muscle Disease Unit, National Institute of Arthritis and Musculoskeletal and Skin Diseases, National Institutes of Health, Bethesda, MD, USA; ⁹Faculty of Health Sciences and Faculty of Computer Science, Multimedia, and Telecommunications, Open University of Catalonia, Barcelona, Spain; ¹⁰Solomon H. Synder Department of Neuroscience, Johns Hopkins University School of Medicine, Baltimore, MD, USA; ¹¹Institute of Medical Genomics, International University of Health and Welfare, Chiba, Japan; ¹²Department of Physical Therapy, Tokyo University of Technology, Tokyo, Japan; ¹³Department of Neurology, International University of Health and Welfare, Mita Hospital, Tokyo, Japan; and ¹⁴Department of Neurology, International University of Health and Welfare, Ichikawa Hospital, Chiba, Japan

Additional supporting information can be found in the online version of this article.

Inclusion body myositis (IBM) is the most common myopathy among people older than 50 years.^{1,2} Patients with IBM typically present with slowly progressive weakness affecting both proximal and distal muscles with a predilection for wrist and finger flexors and/or knee extensors.^{1–3} The skeletal muscles of IBM patients are affected by both inflammation, including CD8-positive T cells invading myofibers, and degeneration, including fibers with abnormal protein aggregation and vacuolation.^{2,3} Although various contributory factors have been reported, the pathogenesis of IBM remains unclear, and there is no established treatment.^{2–5}

Previous studies have reported various abnormalities in the muscle of IBM patients, including overproduction of immune protein transcripts,⁶ widespread changes in the pathways related to RNA metabolism,⁷ intracellular calcium ion dysregulation,⁸ and differentially expressed long non-coding RNAs related to muscle proliferation and differentiation.⁹ The expression levels of the type I interferon-inducible genes in the muscle of patients with IBM were lower compared with those in the muscle of patients with active dermatomyositis or antisynthetase syndrome.¹⁰ The expression levels of type II interferon-inducible genes in muscle were high in IBM muscle biopsies.¹⁰ Using machine learning algorithms, high expression levels of *MYH4* and *JCHAIN*, in addition to the low expression level of *H19*, a non-coding RNA, were shown to be characteristic of muscle from patients with IBM.¹¹ Laser microdissection analysis of muscle fibers revealed differential upregulation of the interferon- γ signaling cascade in the myofibers surrounded and invaded by CD8-positive T cells.¹² Additionally, the protein levels of many fast-twitch specific structural proteins were decreased despite relative preservation of transcript levels in the muscle of IBM.¹³

Previously, we analyzed the clinicopathological features of patients with IBM and polymyositis (PM), which showed CD8-positive T cells invading non-necrotic muscle fibers expressing major histocompatibility complex class I (CD8-MHC-I) pathology.¹⁴ Using this sample set, we aimed to elucidate the comprehensive molecular features of muscles affected by IBM using RNA sequencing.

Subjects and Methods

Participants and Muscle Biopsy Samples

The muscle biopsy reports of idiopathic inflammatory myopathies from 1993 to 2016 were retrospectively reviewed. Written informed consent was obtained from the participants at the time of the biopsy. The study was approved by the institutional review board (IRB) of the University of Tokyo (IRB number G10072).

There were 58 patients with the CD8-MHC-I pathology whose muscle samples were available for RNA sequencing (Table 1). Among these 58 patients, 43 patients were classified as IBM and 6 patients as PM according to the European Neuromuscular Center (ENMC) diagnostic criteria.^{15,16} There was no significant difference in the age at biopsy between IBM and PM. The 58 patients included 9 patients with unclassifiable myositis, who showed distal muscle weakness other than finger flexor muscle weakness but met neither IBM nor PM ENMC diagnostic criteria.¹⁴ The patients with unclassifiable myositis are different from patients with unspecific myositis in that they show CD8-MHC-I pathology and potentially include patients who may develop the weakness that meets the diagnostic criteria of IBM with further follow-up. Nine muscle biopsy samples from those who were suspected of mitochondrial disorders due to mild ataxia or myoclonus but showed no pathological abnormality were used as controls. We also analyzed the clinical features of the participants as follows; age at onset, duration of disease before biopsy, serum creatine kinase (CK) levels, and the presence of anti-cytosolic 5'-nucleotidase 1A (cN1A) antibody.

The frozen muscle samples used for the immunohistochemical analyses included 22 IBM, 7 PM, 7 unclassifiable myositis with CD8-MHC-I pathology, 10 immune-mediated necrotizing myopathy (IMNM), 8 antisynthetase syndrome, 18 dermatomyositis (10 were positive for anti-Mi-2 antibody, and 3 of them were positive for anti-melanoma differentiation-associated protein 5 antibody), and 9 normal controls. These samples of IBM, PM, and control were also included in the RNA sequencing analysis, except for one sample of a PM patient. The patients with IMNM or dermatomyositis fulfilled the ENMC criteria for the respective diseases.^{15,17} Antisynthetase syndrome was diagnosed by the presence of anti-aminoacyl tRNA synthetase antibody and one or more of the following clinical features: Raynaud phenomenon, arthritis, interstitial lung disease, fever, mechanic's hands, or biopsy finding of immune myopathy with perimysial pathology.^{18–20}

RNA Extraction

Before using the muscle samples for RNA sequencing, C.I. and J.S. inspected the hematoxylin and eosin-stained sections of the muscle samples and confirmed that there were < 1% fibers with ice artifact within each section. Ten frozen muscle slices with 50 μ m thickness, which were kept at -80°C , were homogenized in 0.75 ml of Trizol at 4°C . RNA was isolated using RNeasy Mini Kit (Qiagen, Venlo, the Netherlands). Concentrations of RNA were measured by Nanodrop spectrophotometer (Thermo Fisher Scientific, Waltham, MA). The integrity of RNA was analyzed by Agilent 2100 bioanalyzer (Agilent Technologies, Santa Clara, CA). The RNA integrity numbers of these samples were confirmed to be > 6, and the interquartile ranges were from 7.6 to 8.2.

Sequence libraries were prepared after removal of ribosomal RNA using TruSeq Stranded Total RNA Sample Prep kit with Ribo-Zero Gold (Illumina, San Diego, CA).

TABLE 1. Clinical Features of the Participants in this Study

Clinical Diagnosis/ Classification	Myositis with CD8-MHC-I Pathology, n = 58					Unclassifiable Myositis With CD8-MHC-I Pathology ^a	Control
	Inclusion Body Myositis, n = 43		Clinically Defined	Probable	Polymyositis		
	Clinicopathologically Defined						
Participants, n	31	9	3	6	9	9	
Sex, M/F	21/10	1/8	1/2	3/3	1/8	5/4	
Age at onset, yr ^b	60 ± 13	70 ± 7.8	65 ± 5.9	62 ± 8.4	61 ± 9.0	N/A	
Age at biopsy, yr ^b	68 ± 8.8	75 ± 7.1	70 ± 3.2	65 ± 8.1	64 ± 10	49 ± 17	
Duration from onset to biopsy, yr ^b	7.7 ± 8.6	5.0 ± 3.8	5.8 ± 3.7	3.2 ± 2.7	2.9 ± 2.6	N/A	
Dysphagia	11/31 (35%)	2/9 (22%)	1/3 (33%)	2/6 (33%)	2/9 (22%)	0	
Finger flexion weakness [> shoulder abduction weakness]	25/31 (81%)	9/9 (100%)	2/3 (67%)	0	0	0	
Knee extension weakness [≥ hip flexion weakness]	26/31 (84%)	9/9 (100%)	1/3 (33%)	0	0	0	
Creatine kinase, IU/l ^b	813 ± 744	552 ± 347	1,445 ± 1,676	830 ± 601	654 ± 316	78 ± 27	
Anti-cytosolic 5'- nucleotidase 1A antibody ^c	9/29 (31%)	3/9 (33%)	1/3 (33%)	0	4/6 (67%)	0	
Muscle biopsy sites	Biceps	18	3	2	0	5	8
	Deltoid	0	0	0	3	0	0
	Quadriceps	12	4	1	1	4	1
	Others	1	2	0	2	0	0
Fiber with rimmed vacuoles	31	0	0	0	1	0	

^aAmong the patients with CD8-MHC-I pathology, patients with unclassifiable myositis showed distal muscle weakness that did not meet the diagnostic criteria of inclusion body myositis.¹⁴

^bMean ± standard deviation.

^cAnti-cytosolic 5'-nucleotidase 1A antibody testing was performed using enzyme-linked immunoassay.

CD8-MHC-I = CD8-positive T cells invading non-necrotic muscle fibers expressing major histocompatibility complex class I; F = female; M = male; N/A = not available.

RNA Sequencing

We used 67 samples (43 IBM, 6 PM, 9 unclassifiable myositis with CD8-MHC-I pathology, and 9 controls) for the RNA sequencing analysis. Using an Illumina HiSeq 2500 machine, 101 bp paired-end sequencing was performed. The qualities of the resulting fastq files were tested using FastQC (v0.11.5), and the reads were aligned to the reference genome (hg38) using R (v3.3.3) and its package Rsubread (v1.24.2).²¹

Statistical Analysis of RNA Sequencing

For counting reads, we used the featureCounts function in the Rsubread package. Group average clustering and principal component analysis (PCA) on the correlation matrix were performed using the Bioconductor package (edgeR and limma).^{22,23}

Differentially expressed genes (DEGs) were detected by the exact test method in edgeR. Expression levels of the 127 genes that had been previously reported in studies and reviews were also analyzed.^{2-12,24-36}

Kyoto Encyclopedia of Genes and Genomes (KEGG) pathway enrichment analysis was performed using *kegg* function in *edgeR* and the CRAN package (*pathfindR*).^{22,37} We determined that the results of KEGG pathway analysis using Wilcoxon rank sum test were statistically significant when *p* values were < 0.01.

Correlations of *CDH1* expression levels with clinical features of IBM (age at onset, duration, and serum CK levels) and expression levels of the other genes were assessed by Spearman's rank correlation coefficients. Correlations of *CDH1* expression levels with the presence of dysphagia, finger flexion weakness, knee extension weakness, and anti-cN1A antibody were assessed by Wilcoxon rank sum test.

Validation of the Expression Level of CDH1 in IBM by the RNA Sequencing Dataset of Idiopathic Inflammatory Myopathies from Previous Publications

To validate the expression level of *CDH1* in the muscle of patients with IBM, we analyzed the independent RNA sequencing dataset of idiopathic inflammatory myopathies.^{10,11} The dataset was derived from the muscle biopsies of 13 IBM, 49 IMNM, 18 antisynthetase syndrome, and 39 dermatomyositis patients, as well as 20 controls. The RNA sequencing dataset was used for the previous publications; however, the dataset was newly analyzed, and the expression data of *CDH1* in this study have not been published before.^{10,11} Correlations of the expression levels of *CDH1* with those of the other genes were assessed by Spearman rank correlation coefficients. The study was approved by the IRBs of the National Institutes of Health (IRB number 91-AR-0196), the Johns Hopkins Myositis Center (IRB number NA_00007454), and the Vall d'Hebron Hospital (Barcelona; IRB number PR[AG] 68/2008).

Immunoprecipitation and Western Blotting

Frozen muscle tissues from 3 controls and 6 IBM patients were used. Muscle tissues were homogenized in Tris-buffered saline (TBS; 50 mM Tris-HCl pH 7.4, 150 mM NaCl) supplemented with Protease Inhibitor Cocktail (Nacalai Tesque, Kyoto, Japan), and then solubilized with 1% NP-40 and 1% Triton X-100 at 4°C for 1 h. The samples were centrifuged at 20,000 × *g* for 10 min. The supernatants (whole cell lysates) were collected, and their protein concentrations were measured using Lowry protein assay kit (Bio-Rad Laboratories, Hercules, CA).

We were not able to detect the bands of cadherin 1 in whole cell lysates of muscle tissue. We assumed that muscle fibers expressing cadherin 1 were not abundant and the concentration of cadherin 1 in the whole muscle tissue lysates was not enough to be detected by the conventional Western blotting. Therefore, we performed enrichment by immunoprecipitation. The supernatant containing 4 mg of protein was precleared by incubating with 20 μl of protein G sepharose beads (GE Healthcare, Pittsburgh, PA) for 90 min at 4°C. After removal of the beads, 0.7 μg of anti-cadherin 1 antibody (67A4, Santa Cruz Biotechnology, Dallas, TX) and 10 μl of protein G sepharose beads were added and incubated overnight at 4°C.

The beads were washed 3 times with 0.1% NP-40 and 0.1% Triton X-100 containing TBS, and bound materials were eluted by boiling at 95°C for 3 min in Laemmli sample buffer.

For Western blotting, equal amounts of immunoprecipitated samples were subjected to 4 to 15% sodium dodecyl sulfate-polyacrylamide gradient gel electrophoresis (Bio-Rad Laboratories) and proteins were transferred to polyvinylidene difluoride membranes (Merck Millipore, Burlington, MA). After blocking with 5% nonfat dry milk (Nacalai Tesque) in TBS with 0.1% Tween-20 (TBS-T) for 1 h, the blotted membranes were incubated with anti-cadherin 1 antibody (1:1,000, BD Biosciences, San Jose, CA) in 5% nonfat dry milk in TBS-T at 4°C overnight. After washing with 5% nonfat dry milk in TBS-T, the membranes were incubated with anti-mouse IgG2a antibody conjugated with horseradish peroxidase (1:3,000, Jackson ImmunoResearch Laboratories, West Grove, PA) for 1 h at room temperature. After washing with TBS-T, protein bands were visualized by the ECL Prime Western blotting detection system (GE Healthcare, Madison, WI). Whole cell lysates of human prostate cancer cell line PC-3 (American Type Culture Collection, Manassas, VA) were used as a positive control for cadherin 1. Anti-caveolin 3 antibody (1:1,000, Abcam, Cambridge, UK) was used as an internal control to confirm that equal amounts of protein were subjected to immunoprecipitation.

Immunohistochemistry

Serial frozen muscle sections from 22 IBM, 7 PM, 10 IMNM, 8 antisynthetase syndromes, and 18 dermatomyositis cases and 9 normal controls with 10 μm thickness were used for immunohistochemistry. The sections were fixed with 100% acetone and methanol, which contained 4% hydrogen peroxide, followed by blocking by 10% normal goat serum in phosphate-buffered saline. Then, these sections were incubated overnight at 4°C with the primary antibodies against cadherin 1 (E-cadherin [67A4], 1:100, Santa Cruz Biotechnology) or sequestosome 1 (p62 [D3], 1:1,000, Santa Cruz Biotechnology), which were diluted with the blocking solutions. The sections were incubated with biotinylated antimouse immunoglobulin G antibodies (Vector Laboratories, Burlingame, CA). The avidin-biotin complex method with 3,3'-diaminobenzidine was performed for visualization. We called the staining pattern "diffuse" when the cytoplasm of muscle fibers was diffusely stained without granular aggregates.

Analysis of Human Skeletal Muscle Cell Culture and Mouse Muscle Injury

To validate the expression level of *CDH1* during skeletal muscle differentiation and regeneration, we used the RNA sequencing datasets of proliferating human myoblasts and mouse muscle regeneration in the previous reports and analyzed newly.¹¹ In the former experiment, normal human skeletal muscle myoblasts (Lonza, Basel, Switzerland) were cultured according to the manufacturer's protocol. When 80% confluent (day 0), the cultures were placed in differentiation media (Dulbecco modified Eagle medium, 2% horse serum, and L-glutamine) and allowed to differentiate into myotubes. Two plates of cells were collected for

RNA extraction over the next 6 days. In the latter experiment, 6-week-old C57BL/6 mice were unilaterally injured by intramuscular injection of 0.1 ml of 10 μ M cardiotoxin into the tibialis anterior (TA) muscle. Injured TA muscles and uninjured contralateral TA muscles were harvested at subsequent time points for transcriptomic analysis.

Data Availability

The data that support the findings of this study are available in the Japanese Genotype-Phenotype Archive (JGAS000068) at DNA Data Bank of Japan.

Results

Among the 28,395 genes, we analyzed the expression levels of 27,447 genes whose expressions were detected. To assess the effect of biopsy sites, the following muscle

biopsy samples of IBM were compared: 17 biceps and 9 quadriceps biopsies. The pathological findings were similar regardless of the biopsy site. KEGG pathway enrichment analysis showed no significantly upregulated or downregulated pathways in both biopsy sites, albeit the expression of *MYL6B* in biceps was 3 times higher than in quadriceps and the expression of *MYH11* and *MYH4* in quadriceps was 4 times higher than in biceps. PCA on 23 biceps and 17 quadriceps biopsies in IBM confirmed that the two groups are indistinguishable.

Comprehensive Analysis of Gene Expression

Cluster analysis and PCA of all the muscle samples revealed that the diseased muscles were significantly different from the controls (Fig 1A, B). However, none of the 3 clinicopathological groups—IBM, PM, and unclassifiable myositis

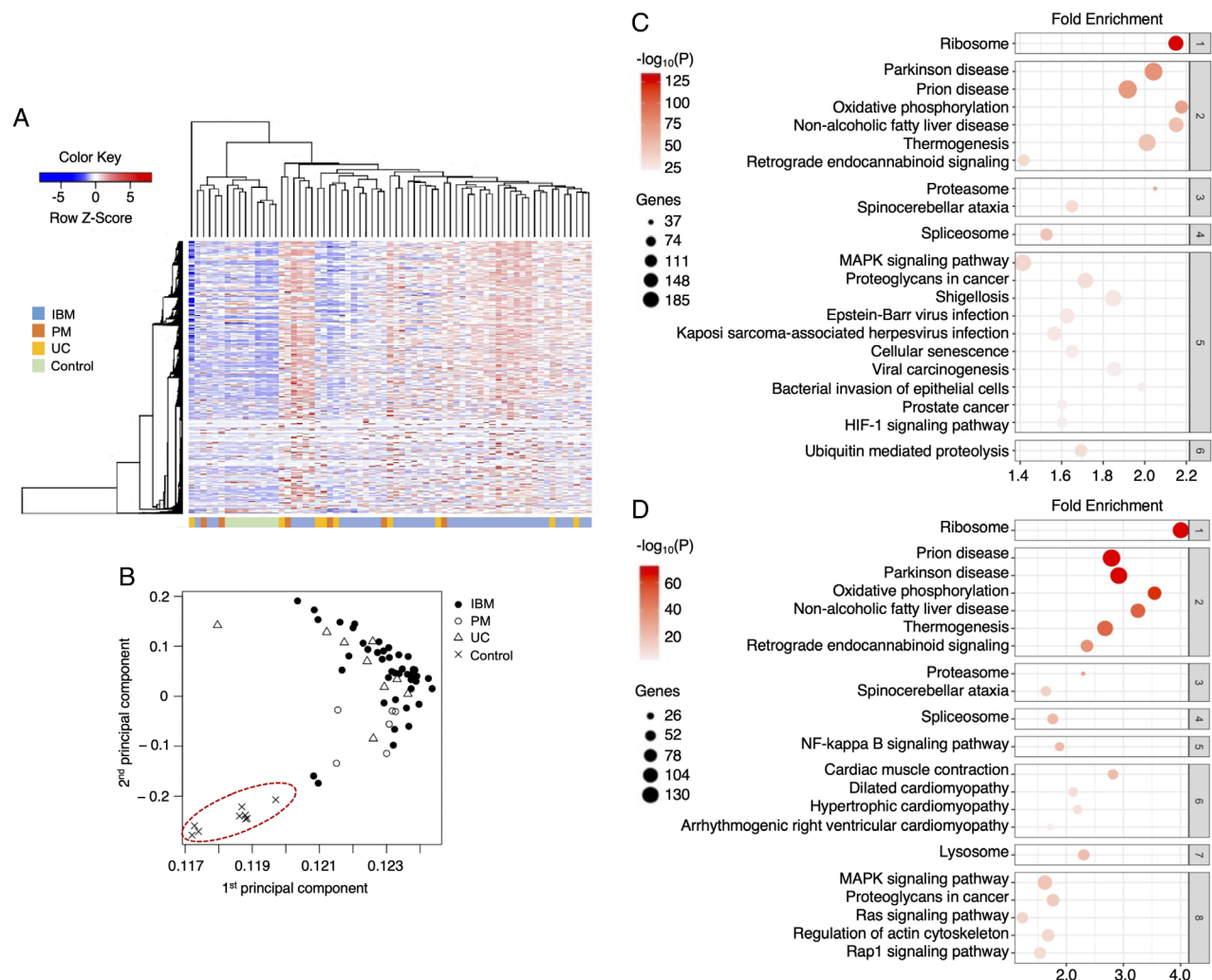


FIGURE 1: Comprehensive analysis of gene expression in skeletal muscle. (C, D) Average linkage cluster analysis (A) and principal component analysis (B) using the RNA sequencing dataset of the patients with CD8-positive T cells invading non-necrotic muscle fibers expressing major histocompatibility complex class I pathology, which included inclusion body myositis (IBM), polymyositis (PM), and unclassifiable myositis (UC). We also included 9 muscle biopsy samples without pathological abnormality as controls. Red dashed oval delineates cluster of controls. (C, D) Kyoto Encyclopedia of Genes and Genomes pathway analysis of IBM (C) and that of PM (D).

with CD8-MHC-I pathology—was distinct from the others. The cumulative proportion of the second principal component of PCA was 97%, meaning that 97% of the difference between clusters can be explained by the first 2 principal components of PCA. The 3 clinicopathological groups (IBM, PM, and unclassifiable myositis with CD8-MHC-I pathology) were not differentiated by the first or second principal components of PCA.

Detection of Differentially Expressed Genes and KEGG Pathway Analysis

On the basis of the result that the diseased muscles were significantly different from the controls in the cluster analysis and PCA, we performed KEGG pathway analysis. Compared with the controls, there were 7,627 DEGs in IBM and 2,803 DEGs in PM, among which 2,741 DEGs were shared (false discovery rate [FDR] < 0.01). Compared with histologically normal controls, the pathways related to oxidative phosphorylation and protein synthesis (described as pathways of ribosomes) were downregulated, whereas pathways of cell adhesion molecules, which were included in the pathways of cancer and infection, were upregulated in the samples of IBM, PM, and unclassifiable myositis with CD8-MHC-I pathology (see Fig 1C, D).

The direct comparison between IBM and PM showed that there were 1,743 DEGs (FDR < 0.05) in IBM, and the FDRs of 411 DEGs were < 0.01. Among the 1,743 DEGs (FDR < 0.05), the expression levels of 30 genes in IBM were at least 8 times higher than those in PM, and 16 of them coded for immunoglobulins. Among the 411 DEGs (FDR < 0.01), there were 38 genes whose expression levels in IBM were at least 2 times higher than those in PM. Among the 38 genes, *CDH1* (cadherin 1; also known as epithelial cadherin, E-cadherin, or CD324) was included. *CDH1* was markedly more expressed in IBM than in control and PM muscle biopsies (Fig 2A).

There were differences of upregulated pathways and downregulated pathways when the dataset of IBM was compared with that of PM. Pathways related to protein processing in the endoplasmic reticulum, cell death, nuclear factor-kappa B signaling pathway, and cell adhesion molecules were upregulated in IBM as compared to PM. Pathways related to the endocrine system, Erb-B2 receptor tyrosine kinase, adenosine monophosphate-activated protein kinase, forkhead box O, cyclic adenosine monophosphate, calcium signaling, and autophagy were downregulated in IBM as compared to PM ($p < 0.01$).

Correlation Analysis with the Expression Level of CDH1 in IBM

There were no clear correlations between the expression level of *CDH1* and the clinical features of IBM patients.

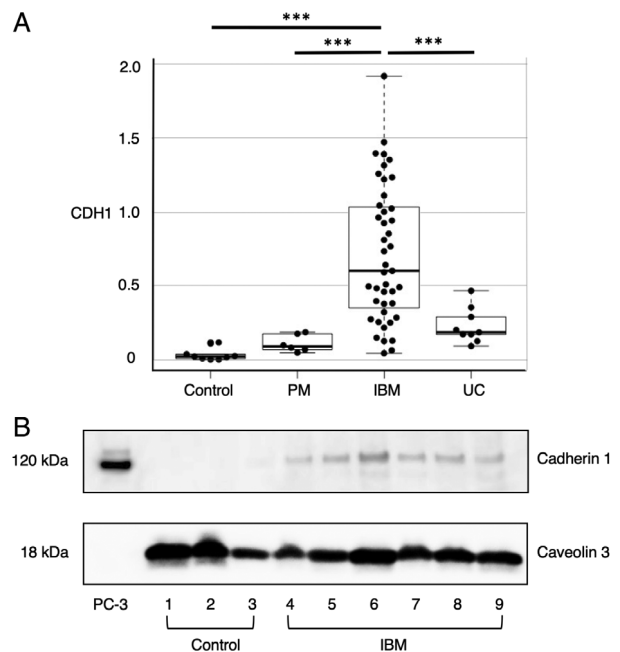


FIGURE 2: Expression of cadherin 1 in skeletal muscle. (A) Transcripts of *CDH1* (\log_2 reads per kilobase per million + 1) in the patients with CD8-positive T cells invading non-necrotic muscle fibers expressing major histocompatibility complex class I pathology, which included inclusion body myositis (IBM), polymyositis (PM), and unclassifiable myositis (UC). We also included 9 controls. *** $p < 0.001$. (B) Western blotting. Lanes 1 to 3: controls. Lanes 4 to 9: IBM. PC-3 = prostate cancer cell line.

The Spearman rank correlations were not significant for age at onset ($\rho = -0.19$), duration ($\rho = 0.04$), and serum CK levels ($\rho < 0.01$). Wilcoxon rank sum tests did not show statistical significance for the presence of dysphagia ($p = 0.69$), finger flexion ($p = 0.43$), knee extension weakness ($p = 0.99$), and anti-cN1A antibody ($p = 0.84$).

Screening of correlations between the expression levels of *CDH1* and other genes showed that there was no gene with a significantly negative correlation. However, there were 236 genes whose Spearman's correlation coefficients were > 0.7 (very strong positive correlation). Among them, the correlation coefficients were > 0.8 with 20 genes (Table S1). For some of these genes, physiological correlations with cadherin 1 have already been reported. *AJUBA* ($\rho = 0.84$) encodes LIM domain-containing protein ajuba, which interacts with alpha-catenin at cadherin adhesive complexes.³⁸ *DNMT3B* ($\rho = 0.83$) is a DNA methyltransferase that binds to the *CDH1* promoter region and regulates the expression of *CDH1*.³⁹ The expression levels of the genes that have been reported in previous studies and their correlations with *CDH1* were also assessed. Cadherin 1 is a ligand of killer cell lectinlike receptor G1 (KLRG1), which was reported to be present on T cells invading IBM muscle.^{34,40} There was no or negligible correlation between the expression of *KLRG1* and that of *CDH1*, although the expression

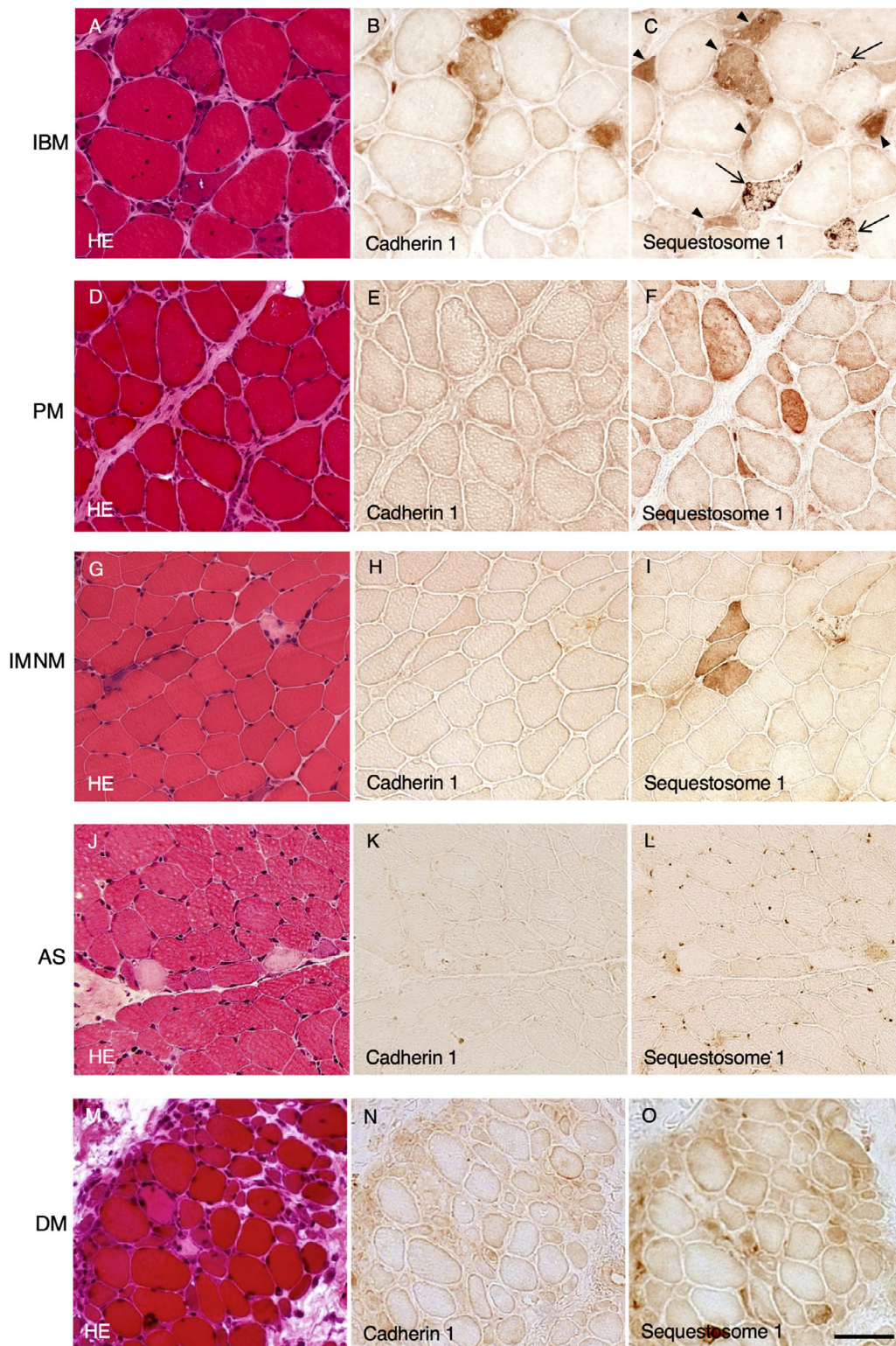


FIGURE 3: Immunohistochemical analysis of idiopathic inflammatory myopathies. Serial sections of inclusion body myositis (IBM; A–C), polymyositis (PM; D–F), immune-mediated necrotizing myopathy (IMNM; G–I), antisynthetase syndrome (AS; J–L), and dermatomyositis (DM; M–O). Hematoxylin and eosin (HE) staining (A, D, G, J, and M), anti-cadherin 1 antibody staining (B, E, H, K, and N), and anti-sequestosome 1 antibody staining (C, F, I, L, and O) were used. Arrowheads in C present fibers stained diffusely with anti-sequestosome 1 antibody. Arrows in C present fibers containing sequestosome 1-positive dense aggregates. In IBM, the muscle fibers stained with anti-cadherin 1 antibody were diffusely stained with anti-sequestosome 1 antibody, whereas those with rimmed vacuoles and/or dense sequestosome 1-positive aggregates were hardly stained with anti-cadherin 1 antibody. In PM, IMNM, AS, DM, and controls, cadherin 1-positive fibers were hardly or not at all detected, as summarized in the Table 2. Scale bar = 100 μ m (applies to all parts).

TABLE 2. Immunohistochemical Analysis of Cadherin 1

Pathology	Total Samples, n	Cadherin 1-Positive Samples, n	Observations
Inclusion body myositis	22	15 (68%)	Diffusely stained fibers were scattered (5–10% of muscle fibers per section)
Polymyositis	7	1 (14%)	Diffusely stained fibers were scattered (a few muscle fibers per section)
Unclassifiable myositis with CD8-MHC-I pathology ^a	7	2 (29%)	Diffusely stained fibers were scattered (a few muscle fibers per section)
Immune-mediated necrotizing myopathy	10	0	No fiber was stained
Antisynthetase syndrome	8	0	No fiber was stained
Dermatomyositis	18	1 (6%)	Two fibers per section were stained diffusely
Control	9	0	No fiber was stained

^aAmong the patients with CD8-MHC-I pathology, patients with unclassifiable myositis showed distal muscle weakness that did not meet the diagnostic criteria of inclusion body myositis.
CD8-MHC-I = CD8-positive T cells invading non-necrotic muscle fibers expressing major histocompatibility complex class I.

level of *KLRG1* was upregulated in IBM compared with controls ($p < 0.01$). The type II interferon-induced genes including *GBP1*, *GBP2*, and *PSMB8* were upregulated in IBM compared with control. However, there was no correlation between the expression of these genes and that of *CDH1*.

There was no significant difference between IBM and the controls as to the expression levels of genes encoding

proteins in IBM-associated sarcoplasmic aggregates including *SQSTM1*, *TARDBP*, *HNRNPA1*, and *HNRNPA2B1*. There were moderate or strong positive correlations between the expression of these genes and that of *CDH1*.

The expression levels of genes associated with muscle regeneration including *NCAM1*, *MYOG*, *MYH3*, and *MYH8* were upregulated in IBM, and their correlations with *CDH1* were moderate to very strong.

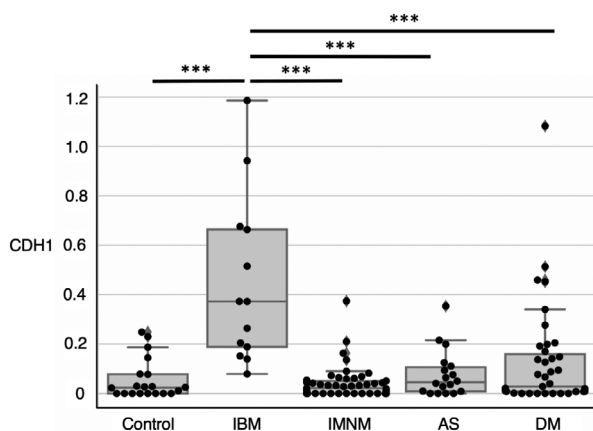


FIGURE 4: The expression of *CDH1* in the RNA sequencing dataset of idiopathic inflammatory myopathies from previous publications. We used the RNA sequencing dataset of idiopathic inflammatory myopathies from previous publications.^{10,11} The expression of *CDH1* (\log_2 [fragments per kilobase per million mapped reads + 1]) in inclusion body myositis (IBM) was compared with those of immune-mediated necrotizing myopathy (IMNM), antisynthetase syndrome (AS), dermatomyositis (DM), and controls. *** $p < 0.001$.

Analysis of Cadherin 1 Protein

To investigate whether cadherin 1 protein was present in the muscle of IBM, Western blotting was performed after immunoprecipitation (see Fig 2B). The expression levels of *CDH1* of the samples that were used for Western blotting were as follows: the 3 control samples were 0.004 reads per kilobase per million (RPKM), 0.064 RPKM, and 0.073 RPKM, and the 6 IBM samples were 0.48 RPKM, 0.88 RPKM, 0.91 RPKM, 0.95 RPKM, 0.96 RPKM, and 1.07 RPKM. *CDH1* protein was detected in all 6 samples from IBM patients but not in any of the control samples. The size of the positive band was 120 kDa, which is the size of the mature cadherin 1 molecule.

The histological study revealed the distribution of the muscle fibers expressing cadherin 1, infiltration of inflammatory cells, and degenerative fibers with rimmed vacuoles and sequestosome 1-positive aggregates. Fifteen of 22 IBM samples (68%) showed a scattered distribution of muscle fibers stained diffusely with anti-cadherin 1 antibody (Fig 3,

TABLE 3. Analysis of Correlation with CDH1 Expression in Inclusion Body Myositis

Gene ^a	Fold Change Compared with Controls (Wilcox test <i>p</i>)		Spearman's Correlation Coefficient (<i>p</i>)	
Interacting with <i>CDH1</i>				
<i>KLRG1</i>	4.033	(4.566E-07)	0.179	(2.515E-01)
INF2-induced genes				
<i>GBP1</i>	20.487	(1.033E-08)	-0.116	(4.595E-01)
<i>GBP2</i>	5.922	(1.441E-07)	-0.080	(6.109E-01)
<i>PSMB8</i>	13.494	(4.311E-06)	-0.015	(9.230E-01)
Markers of sarcoplasmic protein aggregates				
<i>SQSTM1</i>	0.790	(1.272E-02)	0.330	(3.085E-02)
<i>TARDBP</i>	1.185	(1.708E-01)	0.667	(1.044E-06)
<i>HNRNPA1</i>	1.243	(6.425E-02)	0.435	(3.541E-03)
<i>HNRNPA2B1</i>	0.912	(5.047E-01)	0.335	(2.815E-02)
Regeneration				
<i>NCAM1</i>	9.035	(5.436E-10)	0.586	(3.611E-05)
<i>MYOG</i>	1.691	(2.563E-03)	0.626	(7.237E-06)
<i>MYH3</i>	2.904	(4.292E-04)	0.389	(9.943E-03)
<i>MYH8</i>	9.877	(3.160E-02)	0.738	(1.619E-08)

The list of genes whose correlation coefficients were >0.8 are shown in Supplementary Table S1.

^aGene symbols are according to the HUGO Gene Nomenclature Committee (<https://www.genenames.org/>). Approved names are listed in Supplementary Table S2.

Table 2). When these staining patterns were compared with those of anti-sequestosome 1 antibody, all the muscle fibers stained with anti-cadherin 1 antibody were diffusely stained with anti-sequestosome 1 antibody (arrowheads in Fig 3C). However, muscle fibers with rimmed vacuoles and/or dense sequestosome 1-positive aggregates were hardly stained with anti-cadherin 1 antibody (arrows in Fig 3C).

No muscle fibers were stained with anti-cadherin 1 in the samples of IMNM (n = 10), antisynthetase syndrome (n = 8), or control (n = 9). There were muscle fibers that were stained diffusely with anti-cadherin 1 in 1 sample of the 7 samples of PM and 2 samples of the 7 samples of unclassifiable myositis with CD8-MHC-I pathology. A few perifascicular fibers were positive in 1 of the 18 samples from patients with dermatomyositis.

Analysis of CDH1 Expression in the Independent RNA Sequencing Dataset of Idiopathic Inflammatory Myopathies

We analyzed the RNA sequencing dataset of skeletal muscle from patients with idiopathic inflammatory myopathies that

were reported previously.^{10,11} The expression level of *CDH1* in the skeletal muscle of IBM was higher than that of IMNM, antisynthetase syndrome, dermatomyositis, or controls ($p < 0.01$; Fig 4). When IBM was compared with control in the dataset, there were 2,204 DEGs whose FDR was < 0.01 . Among them, 1,828 genes (83%) were overlapped with the DEGs in the dataset of the University of Tokyo. There were 385 genes whose Spearman correlation coefficients with *CDH1* were > 0.8 . Spearman correlation coefficients of 39 genes among them were > 0.7 in the dataset of the University of Tokyo, and 9 genes were > 0.8 . Among the genes in Table 3 and Table S1, Spearman's rank correlation coefficients of the following genes were > 0.7 : *COLCA1* ($\rho = 0.780$), *SERPINB12* ($\rho = 0.874$), *CDK15* ($\rho = 0.777$), *AJUBA* ($\rho = 0.882$), *TP53I3* ($\rho = 0.894$), *COL15A1* ($\rho = 0.894$), *DAAMI* ($\rho = 0.774$), *LRTM1* ($\rho = 0.800$), *ELL3* ($\rho = 0.905$), *DNMT3B* ($\rho = 0.843$), *CLSTN2* ($\rho = 0.816$), *ARHGAP28* ($\rho = 0.860$), *TARDBP* ($\rho = 0.753$), *MYOG* ($\rho = 0.700$), and *MYH8* ($\rho = 0.837$). *TARDBP* encodes TAR DNA-binding protein 43 (TDP-43), which is involved in IBM-associated sarcoplasmic aggregates.

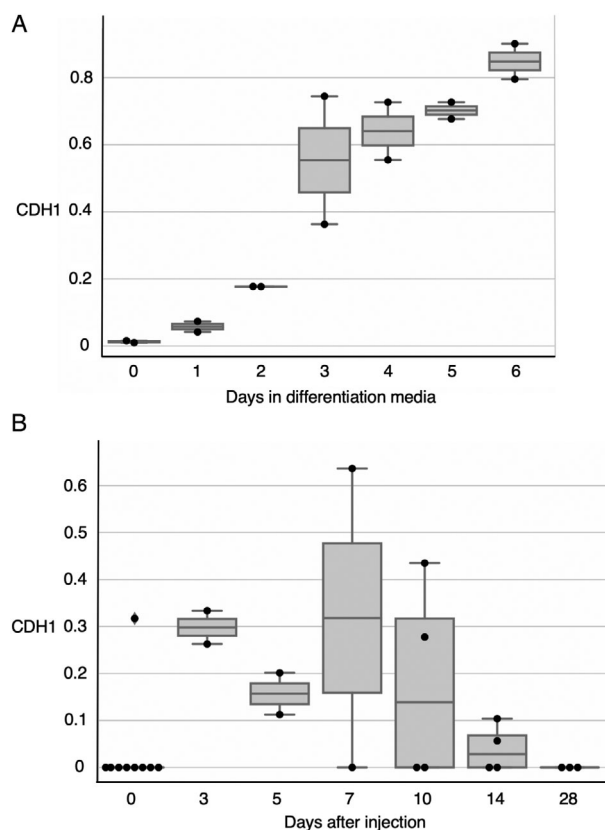


FIGURE 5: The expression of *CDH1* in the experimental systems of muscle differentiation and regeneration. We used the RNA sequencing datasets of proliferating human myoblasts (A) and cardiotoxin injected mouse muscle (B) from previous publications.¹¹ Proliferating human myoblasts were placed in differentiation media on day 0 and allowed to differentiate into myotubes over the next 6 days. In the latter, cardiotoxin was injected into the tibialis anterior muscle of 30 C57BL/6 mice, and muscles were harvested at subsequent time points for transcriptomic analysis.

CDH1 Expression in Skeletal Muscle Differentiation and Regeneration

The expression levels of *CDH1* were also analyzed using the RNA sequencing datasets of proliferating human myoblasts and cardiotoxin-injured skeletal muscle of C57BL/6 mice that were reported previously.¹¹ The expression levels of *CDH1* were upregulated in both experimental systems (Fig 5). In the cardiotoxin-injured mice, the expression level of *CDH1* rose and was shown to peak at 7 days after the injection. Then, it returned to zero at 28 days after cardiotoxin injection into the skeletal muscle of mice (see Fig 5B).

Discussion

This is the largest transcriptomic study of muscle samples from patients with IBM. IBM, PM, and unclassifiable myositis with CD8-MHC-I pathology were not differentiated by cluster analysis or PCA. The results suggest that the

transcriptomic changes among the muscle with the pathological finding of CD8-MHC-I were similar to each other.

In the IBM muscle samples of this study, pathways related to the immune system, immune diseases, and infections were upregulated, and the genes of immunoglobulins were overproduced compared with those in control. For example, among the 30 DEGs whose expression levels were 8 times higher than those in PM, 16 DEGs coded for immunoglobulins.

These results confirmed the previous transcriptomic analyses by microarray, which described the overexpression of immunoglobulin genes including *IGHG3*.⁶ In this study, the expression levels of type II interferon-inducible genes such as *GBP1*, *GBP2*, and *PSMB8* were high in IBM compared with controls, confirming the previous reports.^{10,11} Our study also showed pathways of translation (RNA transport, protein synthesis) and transcription (spliceosome) were downregulated in muscles affected by IBM compared with control muscles. These results supported a previous study that suggested widespread IBM-specific changes in RNA metabolism using samples from 6 patients with IBM.⁷

This study demonstrated the overexpression of *CDH1* in the skeletal muscle of IBM and confirmed the presence and the localization of CDH1 protein by Western blotting and immunohistochemical analyses. Cadherin 1 is a calcium-dependent cell-cell adhesion molecule, which interacts with other cadherin molecules at intercellular boundaries.^{41,42} It is normally expressed in the basolateral membrane of epithelial cells but not in muscle.^{42,43} Regarding the pathway for the delivery of cadherin 1 to the surface of an epithelial cell, Rab11-mediated recycling endosome is known to regulate its exocytosis.⁴³

Previously, an increased number of T cells expressing *KLRG1* in the blood of patients affected by IBM was reported.³⁴ In this study, the expression level of *KLRG1* was upregulated in IBM muscle compared with control muscle. However, the expression of *CDH1* was not correlated with *KLRG1*. In addition, expressions of type II interferon-induced genes were not correlated with *CDH1*. These results suggest that there is no robust association between the expression of *CDH1* and muscle inflammation.

The skeletal muscle of patients with IBM is characterized pathologically by the presence of rimmed vacuoles and abnormal protein aggregates including sequestosome 1 (p62), TDP-43, heterogeneous nuclear ribonucleoprotein A1, and heterogeneous nuclear ribonucleoproteins A2/B1.^{14,36} In both datasets, the expressions of the genes of these pathological markers appeared to correlate with that of *CDH1*, albeit their expressions were neither upregulated nor downregulated compared with controls. Notably, the correlation between the expression of *CDH1*

and *TARDBP* was strong or very strong in these two datasets. Cadherin 1 upregulation might be related to a degenerative process in the muscles of IBM patients.

Skeletal muscle regeneration is an essential process of repairing muscles that have been injured by various causes including the inflammatory cell infiltrates. *NCAMI*, *MYOG*, *MYH3*, and *MYH8* were upregulated in IBM as shown in a previous report.¹¹ The expression of *CDH1* correlated with that of these genes moderately to very strongly in the two datasets. These results suggest that the expression of *CDH1* could be related to the regeneration of muscle of IBM patients. The expression of *CDH1* was confirmed in proliferating human myoblast cultures and regenerating skeletal muscles of cardiotoxin-injured mice.

Expression of genes known to be expressed during skeletal muscle regeneration was commonly upregulated in various types of inflammatory myopathies including IBM.¹¹ However, the overexpression of cadherin 1 protein in skeletal muscles was characteristic of IBM, which suggests the potential usefulness of cadherin 1 as a diagnostic marker of IBM. Further analysis using samples of other muscle diseases including muscular dystrophies would be necessary to assess the specificity of cadherin 1 for the diagnosis of IBM.

The expressions of *CDH1* were correlated with *TARDBP* strongly or very strongly in the two datasets. During normal skeletal muscle regeneration, TDP-43 forms cytoplasmic amyloidlike oligomeric assemblies, referred to as myo-granules in a previous report.⁴⁴ Although myo-granules are cleared as myofibers mature in normal muscle, increased assembly or decreased clearance of myo-granules was suggested to be the source of cytoplasmic TDP-43 aggregates in IBM muscle.⁴⁴ Cadherin 1 might be involved in a process whereby normal myo-granules evolve into cytoplasmic TDP-43 aggregates in the muscles of IBM patients. Further studies are needed to clarify the role of cadherin 1 in the muscle of IBM.

In summary, we demonstrated for the first time that cadherin 1 is overexpressed in the cytoplasm of myofibers from patients with IBM. Its expression in the muscle of IBM patients was high compared with that of control and other idiopathic inflammatory myopathies. Clarifying the cause and consequences of cadherin 1 upregulation may further our understanding of the pathological mechanisms of IBM.

Acknowledgments

C.I. is supported by the Myositis Association (90097118). J.Y. is supported by the Japan Society for the Promotion of Science (JSPS; Grants-in-Aid for Scientific Research [KAKENHI] 16H06279). J.S. is supported by JSPS

(KAKENHI 19K07956). S.T. is supported by JSPS (KAKENHI 22129001 and KAKENHI 22129002); Ministry of Health, Welfare, and Labor (grants-in-aid H23-Jitsuyoka [Nanbyo]-Ippan-004 and H26-Jitsuyoka [Nanbyo]-Ippan-080); and Japan Agency for Medical Research and Development (AMED; 15ek0108065h0002, 16kk0205001h0001, 17kk0205001h0002, and 17ek0109279h0001). T.T. is supported by JSPS (KAKENHI JP20H00526) and AMED (JP20ek0109456h0001). J.G. is supported by JSPS (KAKENHI JP26461265) and the Ministry of Education, Culture, Sports, Science, and Technology (MEXT KAKENHI JP221S0002).

Author Contributions

C.I., H.D., J.M., H.I., J.S., and J.G. contributed to the conception and design of the study; C.I., H.D., M.K., J.Y., I.P.-F., and J.S. contributed to the acquisition and analysis of the data; C.I., H.D., M.K., J.M., H.I., I.P.-F., A.L.M., T.E.L., S.T., J.S., T.T., and J.G. contributed to drafting the manuscript and figures; all authors read and approved the final manuscript.

Potential Conflicts of Interest

Nothing to report.

References

- Lloyd TE, Mammen AL, Amato AA, et al. Evaluation and construction of diagnostic criteria for inclusion body myositis. *Neurology* 2014;83:426–433.
- Wehl CC, Mammen AL. Sporadic inclusion body myositis—a myodegenerative disease or an inflammatory myopathy. *Neuropathol Appl Neurobiol* 2017;43:82–91.
- Wehl CC. Sporadic inclusion body myositis and other rimmed vacuolar myopathies. *Continuum (Minneapolis)* 2019;25:1586–1598.
- Britson KA, Yang SY, Lloyd TE. New developments in the genetics of inclusion body myositis. *Curr Rheumatol Rep* 2018;20:26.
- Keller CW, Schmidt J, Lünemann JD. Immune and myodegenerative pathomechanisms in inclusion body myositis. *Ann Clin Transl Neurol* 2017;4:422–445.
- Greenberg SA, Sanoudou D, Haslett JN, et al. Molecular profiles of inflammatory myopathies. *Neurology* 2002;59:1170–1182.
- Cortese A, Plagnol V, Brady S, et al. Widespread RNA metabolism impairment in sporadic inclusion body myositis TDP43-proteinopathy. *Neurobiol Aging* 2014;35:1491–1498.
- Amici DR, Pinal-Fernandez I, Mázala DA, et al. Calcium dysregulation, functional calpainopathy, and endoplasmic reticulum stress in sporadic inclusion body myositis. *Acta Neuropathol Commun* 2017;5:24.
- Hamann PD, Roux BT, Heward JA, et al. Transcriptional profiling identifies differential expression of long non-coding RNAs in Jo-1 associated and inclusion body myositis. *Sci Rep* 2017;7:8024.
- Pinal-Fernandez I, Casal-Dominguez M, Derfoul A, et al. Identification of distinctive interferon gene signatures in different types of myositis. *Neurology* 2019;93:e1193–e1204.

11. Pinal-Fernandez I, Casal-Dominguez M, Derfoul A, et al. Machine learning algorithms reveal unique gene expression profiles in muscle biopsies from patients with different types of myositis. *Ann Rheum Dis* 2020;79:1234–1242.
12. Ivanidze J, Hoffmann R, Lochmüller H, et al. Inclusion body myositis: laser microdissection reveals differential up-regulation of IFN- γ signaling cascade in attacked versus nonattacked myofibers. *Am J Pathol* 2011;179:1347–1359.
13. Parker KC, Kong SW, Walsh RJ, et al. Fast-twitch sarcomeric and glycolytic enzyme protein loss in inclusion body myositis. *Muscle Nerve* 2009;39:739–753.
14. Ikenaga C, Kubota A, Kadoya M, et al. Clinicopathologic features of myositis patients with CD8-MHC-1 complex pathology. *Neurology* 2017;89:1060–1068.
15. Hoogendijk JE, Amato AA, Lecky BR, et al. 119th ENMC international workshop: trial design in adult idiopathic inflammatory myopathies, with the exception of inclusion body myositis. *Neuromuscul Disord* 2004;14:337–345.
16. Rose MR, ENMC IBM Working Group. 188th ENMC international workshop: inclusion body myositis. *Neuromuscul Disord* 2013;23:1044–1055.
17. Allenbach Y, Mammen AL, Benveniste O, et al. 224th ENMC international workshop: clinico-sero-pathological classification of immune-mediated necrotizing myopathies. *Neuromuscul Disord* 2018;28:87–99.
18. Bucelli RC, Pestronk A. Immune myopathies with perimysial pathology: clinical and laboratory features. *Neurol Neuroimmunol Neuroinflamm* 2018;5:e434.
19. Connors GR, Christopher-Stine L, Oddis CV, Danoff SK. Interstitial lung disease associated with the idiopathic inflammatory myopathies: what progress has been made in the past 35 years? *Chest* 2010;138:1464–1474.
20. Witt LJ, Curran JJ, Strek ME. The diagnosis and treatment of anti-synthetase syndrome. *Clin Pulm Med* 2016;23:218–226.
21. Liao Y, Smyth GK, Shi W. The subread aligner: fast, accurate and scalable read mapping by seed-and-vote. *Nucleic Acids Res* 2013;41:e108.
22. Robinson MD, McCarthy DJ, Smyth GK. edgeR: a Bioconductor package for differential expression analysis of digital gene expression data. *Bioinformatics* 2010;26:139–140.
23. Ritchie ME, Phipson B, Wu D, et al. Limma powers differential expression analyses for RNA-sequencing and microarray studies. *Nucleic Acids Res* 2015;43:e47.
24. Gang Q, Bettencourt C, Machado PM, et al. Rare variants in SQSTM1 and VCP genes and risk of sporadic inclusion body myositis. *Neurobiol Aging* 2016;47:218.e1–218.e9.
25. Gang Q, Bettencourt C, Machado PM, et al. The effects of an intronic polymorphism in TOMM40 and APOE genotypes in sporadic inclusion body myositis. *Neurobiol Aging* 2015;36:1766.e1–1766.e3.
26. Güttsches AK, Brady S, Krause K, et al. Proteomics of rimmed vacuoles define new risk allele in inclusion body myositis. *Ann Neurol* 2017;81:227–239.
27. Johari M, Arumilli M, Palmio J, et al. Association study reveals novel risk loci for sporadic inclusion body myositis. *Eur J Neurol* 2017;24:572–577.
28. Lindgren U, Roos S, Hedberg Oldfors C, et al. Mitochondrial pathology in inclusion body myositis. *Neuromuscul Disord* 2015;25:281–288.
29. Mastaglia FL, Rojana-udomsart A, James I, et al. Polymorphism in the TOMM40 gene modifies the risk of developing sporadic inclusion body myositis and the age of onset of symptoms. *Neuromuscul Disord* 2013;23:969–974.
30. Rothwell S, Cooper RG, Lundberg IE, et al. Immune-array analysis in sporadic inclusion body myositis reveals HLA-DRB1 amino acid heterogeneity across the myositis spectrum. *Arthritis Rheumatol* 2017;69:1090–1099.
31. Scott AP, Laing NG, Mastaglia F, et al. Investigation of NOTCH4 coding region polymorphisms in sporadic inclusion body myositis. *J Neuroimmunol* 2012;250:66–70.
32. Wehl CC, Baloh RH, Lee Y, et al. Targeted sequencing and identification of genetic variants in sporadic inclusion body myositis. *Neuromuscul Disord* 2015;25:289–296.
33. Panaite PA, Stalder AK, Ipsen S, et al. mTOR is expressed in polymyositis but not in sporadic inclusion body myositis. *Clin Neuropathol* 2015;34:371–373.
34. Greenberg SA, Pinkus JL, Kong SW, et al. Highly differentiated cytotoxic T cells in inclusion body myositis. *Brain* 2019;142:2590–2604.
35. Morosetti R, Broccolini A, Sancricca C, et al. Increased aging in primary muscle cultures of sporadic inclusion-body myositis. *Neurobiol Aging* 2010;31:1205–1214.
36. Pinkus JL, Amato AA, Taylor JP, Greenberg SA. Abnormal distribution of heterogeneous nuclear ribonucleoproteins in sporadic inclusion body myositis. *Neuromuscul Disord* 2014;24:611–616.
37. Ulgen E, Ozisik O, Sezerman OU. pathfindR: an R package for comprehensive identification of enriched pathways in omics data through active subnetworks. *Front Genet* 2019;10:858.
38. Marie H, Pratt SJ, Betson M, et al. The LIM protein Ajuba is recruited to cadherin-dependent cell junctions through an association with alpha-catenin. *J Biol Chem* 2003;278:1220–1228.
39. Kwon O, Jeong SJ, Kim SO, et al. Modulation of E-cadherin expression by K-Ras; involvement of DNA methyltransferase-3b. *Carcinogenesis* 2010;31:1194–1201.
40. Van den Bossche J, Malissen B, Mantovani A, et al. Regulation and function of the E-cadherin/catenin complex in cells of the monocyte-macrophage lineage and DCs. *Blood* 2012;119:1623–1633.
41. Hirano S, Nose A, Hatta K, et al. Calcium-dependent cell-cell adhesion molecules (cadherins): subclass specificities and possible involvement of actin bundles. *J Cell Biol* 1987;105:2501–2510.
42. Nagafuchi A, Shirayoshi Y, Okazaki K, et al. Transformation of cell adhesion properties by exogenously introduced E-cadherin cDNA. *Nature* 1987;329:341–343.
43. Lock JG, Stow JL. Rab11 in recycling endosomes regulates the sorting and basolateral transport of E-cadherin. *Mol Biol Cell* 2005;16:1744–1755.
44. Vogler TO, Wheeler JR, Nguyen ED, et al. TDP-43 and RNA form amyloid-like myo-granules in regenerating muscle. *Nature* 2018;563:508–513.